ACS Infectious Diseases

pubs.acs.org/journal/aidcbc
Article

Bacterial Carbonic Anhydrase Inhibitor CAI0019 Demonstrates Efficacy in *Enterococcus faecium* Septicemic Peritonitis Mouse Model While Sparing the Microbiome

Nader S. Abutaleb,[#] Katrina J. Holly,[#] Carolyn K. Metcalfe, Ahmed A. Abouelkhair, Prabhakara R. Tharra, Annadka Shrinidhi, Abdallah S. Abdelsattar, Victoria Burgo, Glory Melotte, Tomi Akin-Olabiyi, Sean Knoblauch, Ramanujam Ramaswamy, Che Woodson, Venkatesh P. Thirumalaikumar, J. Alejandra Rodriguez, Franklin J. Yeo, Olivia C. Snell, Alessio Nocentini, Anitha Sundararajan, Matthew R. Olson, Claudiu T. Supuran, Mohamed N. Seleem,* and Daniel P. Flaherty*

Cite This: *ACS Infect. Dis.* 2026, 12, 176−189

Read Online

ACCESS | Metrics & More | Article Recommendations | Supporting Information

ABSTRACT: Vancomycin-resistant enterococci are multidrug-resistant bacteria that as of 2021 continue to pervade the U.S. healthcare system as the second-most prevalent source of healthcare-acquired infections behind *Escherichia coli*. Given the limited treatment options for vancomycin-resistant enterococci and growing concerns about antibiotic-induced gut microbiome dysbiosis, there is an urgent need for narrow-spectrum antibiotics that can selectively target vancomycin-resistant enterococci while preserving the integrity of the gut microbiome. Previous studies have demonstrated the in vivo potential of orally dosed acetazolamide-based compounds to reduce vancomycin-resistant enterococci bioburden in the gastrointestinal tract and internal organs of mice. However, while it is hypothesized that these molecules inhibit bacterial carbonic anhydrases, the exact target of the acetazolamide scaffold in vancomycin-resistant enterococci has remained unconfirmed. Additionally, the impact of the scaffold on in vivo gut microbiome diversity remains uncharacterized. The work herein reports the chemoproteomic identification of α-carbonic anhydrase as the primary target of the acetazolamide scaffold in *E. faecium* and presents its uniqueness as a narrow-spectrum antibiotic target that can be exploited by CAI0019, a lead acetazolamide derivative with in vivo efficacy, while sparing gut microbiome diversity in mice. This work presents compelling data that not only confirm α-carbonic anhydrase as an antibiotic target in *Enterococcus* but also demonstrate that narrow-spectrum in vivo antienterococcal efficacy can be achieved through targeting α-carbonic anhydrase such that gut commensal microbiota remain unimpacted.

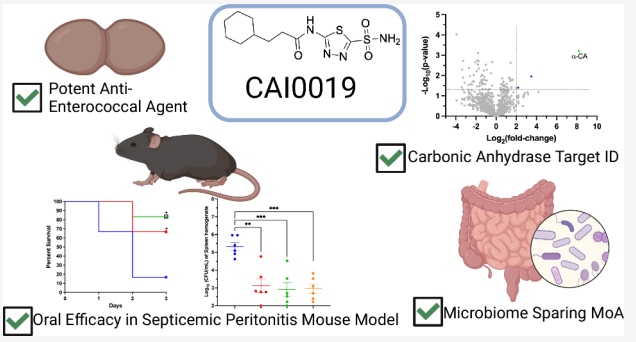

KEYWORDS: *antibiotics, carbonic anhydrase inhibitor, enterococcus, microbiome, chemoproteomics, pharmacokinetics, animal models*

Enterococcus pathogens are among the most prevalent antibiotic-resistance threats in the United States, driven by the rise of vancomycin-resistant *Enterococcus* (VRE), mainly comprised of *E. faecium* and *E. faecalis*.[1] According to the Centers for Disease Control and Prevention, *Enterococcus* species were the second leading cause of hospital-acquired infections behind *Escherichia coli* from 2018 to 2021 in the U.S.[2] VRE is not only a problem in the hospital but a major burden on long-term-healthcare facilities.[3−5] VRE colonization is a critical risk factor for patients in healthcare settings, which is mainly initiated by exposure to antibiotics that create microbial dysbiosis in the gastrointestinal tract (GIT) of a patient and is the origin point for downstream infections.[6,7] There is an urgent need for novel therapeutics to treat *Enterococcus* infections. The current standard-of-care for VRE is either linezolid[8] or off-label use of daptomycin,[8] which suffer from dose-limiting toxicity[9] and disruption of the microbial balance of the microbiome.[10]

With respect to the gut microbiome, dysbiosis in the gut has been linked to many downstream health consequences, including cancer[11,12] and neurodegenerative disease.[13] With respect to *Enterococcus,* it comprises <0.2% of the gut microbiota in healthy humans.[14] However, overgrowth of

Received: August 21, 2025
Revised: December 2, 2025
Accepted: December 4, 2025
Published: December 11, 2025

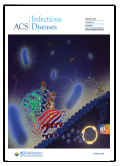

microbiome enterococci bacteria or escape from the GIT can promote both colorectal cancer,[15] autoimmune disorders,[16] and *Clostridioides difficile* infection.[17] The growing understanding of the impact of the gut microbiome on human health has led to an emphasis on considering antibiotic effects on the gut microbiome.[18] This has paved the way for strategies to preserve the microbiome, such as fecal transplant after antibiotic treatment[19] and development of pathogen-specific microbiome-sparing antibiotics.[20,21]

Carbonic anhydrases (CAs) are metalloenzymes that catalyze the conversion of water and carbon dioxide to bicarbonate and a proton mediated through a zinc ion (Zn^{2+}) in the active site. The resulting products are critical for physiological processes such as pH homeostasis, cellular signaling, and metabolic processes.[22] There are a variety of genetically and structurally distinct CA subfamilies, including α-, β-, and γ-classes within bacterial lineages,[23,24] while humans only encode for the α-class of CA.[25] The Food and Drug Administration (FDA)-approved human CA inhibitor acetazolamide, AZM (Figure 1), is commonly prescribed for

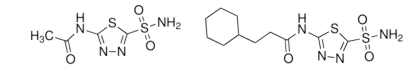

Acetazolamide (AZM)
E. faecium MIC = 4.50 – 18.0 μM
E. faecium α-CA K_i = 56.7 nM
E. faecium γ-CA K_i = 323 nM
Human CA 1 K_i = 250 nM
Human CA 2 K_i = 12.5 nM

CAI0019
E. faecium MIC = 22 – 189 nM
E. faecium α-CA K_i = 66.9 nM
E. faecium γ-CA K_i = 346 nM
Human CA 1 K_i = 946 nM
Human CA 2 K_i = 0.32 nM

Figure 1. Structures of acetazolamide (AZM) and CAI0019 with prior reported antienterococcal activity[29] and biochemical inhibition of bacterial and human carbonic anhydrases.[30]

treatment of altitude sickness,[26] glaucoma,[27] and as a diuretic.[28] Our team has targeted bacterial CAs for antibiotic drug development against *Enterococcus* species[29−34] and *Neisseria gonorrheae*.[35−39] These efforts have led to proof-of-concept results that bacterial CA inhibitors effectively decolonize the GIT of mice from *Enterococcus* infection[40] and that AZM is effective in a mouse model for *Enterococcus* peritoneal infection.[41]

However, the on-target engagement of these molecules with bacterial CAs has yet to be demonstrated. Various essential metabolic processes require bicarbonate to support bacterial growth.[42−45] A prior report using *Escherichia coli* as a model system calculated that the intracellular demand for bicarbonate is so great that it must have a constant supply to grow, which is provided by the α-CA.[46] In *N. gonorrheae*, a hypomorphic β-CA mutant, with a catalytic efficiency 2 orders of magnitude below that of WT-β-CA, requires CO_2 for growth, while the WT grows efficiently in ambient atmosphere without CO_2 supplementation.[47] This suggests there is a threshold of CA activity necessary to supply enough bicarbonate for efficient growth, and if activity drops below that threshold, the bacteria cannot sustain growth. However, CAs are not the only sources of bicarbonate for many bacteria. Most bacteria express dissolved inorganic carbon (DIC) transporters that can provide the cell with exogenous bicarbonate to satisfy the metabolic flux. This was demonstrated in *Staphylococcus aureus* that natively expresses MpsA and MpsB genes, which were shown to be DICs that concentrate bicarbonate into the cell, and it does not possess a CA gene.[48] In fact, Fan et al. carried out an in-depth genomic and phylogenetic analysis of the National Center for Biotechnology Information Reference Sequence Database (RefSeq) and found that *mpsA* and *mpsB* genes are widely distributed in genomes across *Firmicutes*, *Proteobacteria*, *Actinobacteria*, and *Bacteroidetes* phyla.[48] Additionally, the authors also addressed the possibility of species expressing both *mpsAB* and CA and showed that if bacteria coexpress both, MpsAB outperforms the CA in terms of growth restoration during inducible gene expression, and the CA gene is not necessary.[49] Interestingly, it was noted that MpsA and MpsB homologues are not present in *Enterococcus* species among a handful of other human pathogens, and these bacteria only encode for the CA gene. Thus, we hypothesized that targeting bacterial CAs may provide a uniquely narrow-spectrum antibiotic agent that spares the microbiota.

A study was designed that addresses several questions surrounding bacterial CAs as viable antibiotic therapeutic targets. First, we demonstrate intracellular target engagement for the first time against bacterial CAs. Second, we provide proof-of-concept in vivo efficacy in an *Enterococcus* septicemia mouse model after oral dose for the most advanced bacterial CA inhibitor to date, CAI0019 (Figure 1).[29] Last, we sought to evaluate the effect on mouse microbiome diversity upon prolonged oral treatment with CAI0019. The results of these studies are provided herein.

RESULTS AND DISCUSSION

CAI0019 Activity versus a Panel of *Enterococcus* and Other Species Encoding or Lacking MpsAB Homologues. The bacterial CA inhibitor CAI0019 was previously characterized with minimum inhibitory concentration (MIC) values as low as 22 nM against some strains,[29] and potent inhibition of the pathogens' two CAs.[30] In this study, we expanded the *Enterococcus* panel testing from our previous report[29] to include not only additional *E. faecium* and *E. faecalis* strains, but also other clinically relevant strains such as *E. avium*, *E. casseliflavus*, *E. durans*, *E. hirae*, *E. raffinosus*, and *E. saccharolyticus* (Table 1). The data showed that CAI0019 exhibits MICs ranging from 0.022 to 1.57 μM across the panel of 25 *E. faecalis* and *E. faecium* strains, resulting in MIC_{50} (the concentration that inhibited 50% of the strains tested) of 0.094 μM and MIC_{90} (the concentration that inhibited 90% of the strains tested) of 0.39 μM for that subset. This potency was a 96- and 46-fold improvement (for MIC_{50} and MIC_{90}, respectively) compared to the original hit in this series, AZM, with MIC_{50} and MIC_{90} values of 9.01 and 18 μM, respectively. Moreover, the molecule was greater than 31- and 7-fold more potent (MIC_{50} and MIC_{90}) compared to linezolid, which demonstrated MIC_{50} and MIC_{90} of 2.96 μM against the *E. faecalis* and *E. faecium* strains. Intriguingly, the rarer *Enterococcus* strains exhibited a wider range of MIC values for CAI0019, ranging from 0.094 to 50 μM (Table 1), but were still generally more potent compared to AZM (MICs from 2.25 to 72.0 μM). Overall, the MIC_{50} of CAI0019 against all tested *Enterococcus* strains, collectively, was 0.19 μM, a 47-fold improvement over the collective MIC_{50} of AZM and 15-fold more potent than linezolid.

MIC assays were performed in both ambient air conditions and in conditions with 5% CO_2 atmosphere. At 5% CO_2, the level of carbon dioxide is high enough to permeate into the bacterial cell and spontaneously react with water to convert to bicarbonate, making any other bicarbonate-concentrating mechanisms, such as CA, nonessential.[46] Hence, CO_2 supplementation is a way to investigate whether the mechanism of action involves the perturbation of the bicarbonate supply through CA inhibition. Notably, all

https://doi.org/10.1021/acsinfecdis.5c00736
ACS Infect. Dis. 2026, 12, 176−189

Table 1. Minimum Inhibitory Concentrations (MICs) for Molecules against Expanded Panel of *Enterococcus* Isolates and Additional Species

	MIC (μM)					
	CAI0019		AZM		LNZ[a]	
bacterial strain	ambient[b]	CO_2[c]	ambient[b]	CO_2[c]	ambient[b]	CO_2[c]
E. faecalis HM-201	0.39	>200	18.0	>288	2.96	2.96
E. faecalis HM-334[d]	0.022	>200	9.01	>288	2.96	2.96
E. faecalis HM-335[d]	0.094	>200	9.01	>288	1.48	2.96
E. faecalis HM-934	0.39	>200	9.01	>288	2.96	2.96
E. faecalis NR-31970	0.094	>200	18.0	>288	2.96	2.96
E. faecalis NR-31971[d]	0.022	>200	9.01	>288	2.96	2.96
E. faecalis NR-31972[d]	0.047	>200	9.01	>288	1.48	2.96
E. faecium ATCC 700221	0.19	>200	9.01	>288	2.96	2.96
E. faecium HM-952	0.19	>200	9.01	>288	2.96	2.96
E. faecium HM-965	0.022	>200	4.50	>288	2.96	2.96
E. faecium HM-968[d]	0.094	>200	9.01	>288	1.48	2.96
E. faecium HM-970	0.19	>200	9.01	>288	2.96	2.96
E. faecium NR-28978[d]	0.19	>200	9.01	>288	2.96	2.96
E. faecium NR-31903[d]	0.047	>200	9.01	>288	47.4	47.4
E. faecium NR-31909	0.19	>200	9.01	>288	2.96	2.96
E. faecium NR-31912	0.19	>200	9.01	>288	2.96	2.96
E. faecium NR-31914[d]	0.094	>200	9.01	>288	2.96	2.96
E. faecium NR-31916[d]	0.094	>200	9.01	>288	2.96	2.96
E. faecium NR-31933	0.39	>200	9.01	>288	2.96	2.96
E. faecium NR-31937	0.79	>200	9.01	>288	2.96	2.96
E. faecium NR-31954	1.57	>200	36.0	>288	2.96	2.96
E. faecium NR-32052[d]	0.047	>200	9.01	>288	1.48	1.48
E. faecium NR-32053	0.094	>200	4.50	>288	2.96	2.96
E. faecium NR-32065[d]	0.047	>200	4.50	>288	0.74	1.48
E. faecium NR-32094	0.19	>200	9.01	>288	1.48	1.48
E. avium ATCC 14025	12.6	>200	72.0	>288	2.96	2.96
E. casseliflavus ATCC 700327	6.28	>200	72.0	>288	2.96	2.96
E. durans ATCC 11576	0.094	>200	2.25	>288	2.96	2.96
E. gallinarum ATCC 49373	6.28	>200	36.0	>288	2.96	2.96
E. hirae ATCC 10541	50.3	>200	36.0	>288	2.96	2.96
E. raffinosus ATCC 49464	0.19	>200	36.0	>288	2.96	2.96
E. saccharolyticus ATCC 43076	0.19	>200	4.50	>288	2.96	2.96
Ef MIC_{50}[e]	0.094		9.01		2.96	
Ef MIC_{90}[f]	0.39		18		2.96	
All*Enterococci spp.* MIC_{50}[g]	0.19		9.01		2.96	
All*Enterococci spp.* MIC_{90}[h]	6.28		36.0		2.96	
Listeria monocytogenes ATCC 19111[i]	100	>500	72	>500	2.96	2.96
Staphylococcus aureus USA300[j]	>500	>500	>500	>500	1.48	1.48
Staphylococcus epidermidis NRS101[j]	>500	>500	>500	>500	2.96	2.96
Bacillus subtilis ATCC11774[k]	>500	>500	>500	>500	1.48	1.48

[a]LNZ = linezolid. [b]Indicates standard conditions in ambient air at 37 °C. [c]Indicates incubation under 5% CO_2 atmosphere at 37 °C. [d]MICs previously reported by Kaur et al.[29] [e]Minimum inhibitory concentration at which the compound inhibited 50% of the tested *E. faecalis* and *E. faecium* strains. [f]Minimum inhibitory concentration at which the compound inhibited 90% of the tested *E. faecalis* and *E. faecium* strains. [g]Minimum inhibitory concentration at which the compound inhibited 50% of all tested *Enterococcus* strains. [h]Minimum inhibitory concentration at which the compound inhibited 90% of all tested *Enterococcus* strains. [i]*L. monocytogenes* encodes only an α-CA and does not encode for MpsAB homologues. [j]*S. aureus* and *S. epidermidis* do not encode for any CAs and do express MpsAB homologues. [k]*B. subtilis* encodes for both MpsAB and CAs.

Enterococcus species exhibited large shifts in susceptibility in the presence of CO_2 (MICs > 200 and 288 μM for CAI0019 and AZM, respectively) (Table 1), coupled with potent biochemical CA inhibition (Figure 1), indicating that CA inhibition is likely the mechanism of action for CAI0019 and AZM. Alternatively, the strains exhibited no MIC shift with linezolid, which is known to inhibit protein synthesis by targeting the bacterial 50S ribosomal subunit[50] and thus acts independently of bicarbonate-related mechanisms. These data indicate that CAI0019 has the potential to exhibit broad antienterococcal activity with greater potency than linezolid.

Prior literature reported that most bacteria encode for MpsAB bicarbonate transporters and either do not encode for CAs,[48,51] or if CA is coexpressed, the bacteria rely on MpsAB over CA for bicarbonate sourcing.[52,53] To explore this further with CAI0019 and AZM, we tested the activity against bacteria within three groups. The first being another α-CA expressing species that lacks MpsAB, to which *Enterococcus* belongs, but also represented by *Listeria monocytogenes*.[48] Second were two

https://doi.org/10.1021/acsinfecdis.5c00736
ACS Infect. Dis. 2026, 12, 176−189

strains that lack CA homologues and only encode MpsAB bicarbonate transporters represented by *Staphylococcus aureus* and *Staphylococcus epidermidis*.[48] Finally, the third encoding both CA and MpsAB genes represented by *Bacillus subtilis*.[48] CAI0019 and AZM, while less potent than against *Enterococcus*, were able to inhibit the growth of *L. monocytogenes*, and the pathogen was no longer susceptible in 5% CO_2. The lower potency may be due to differences in the CA enzyme or the entry into the cell. Nonetheless, the CA inhibitors do provide measurable activity. Conversely, neither CAI0019 nor AZM demonstrated any measurable antibacterial activity, up to 500 μM, against the MpsAB-containing species. These results support the prior literature suggesting bacteria that only encode for CAs with no MpsAB homologues would be susceptible, while species that encode for MpsAB, with or without a CA gene, would not be susceptible to bacterial CA inhibitors.

Chemoproteomics Target Engagement Assays. While evidence suggests CA inhibition is the likely mechanism of action for the AZM-based antienterococcal activity, there is still a lack of target engagement data to support this or implicate other potential intracellular targets. Therefore, probes were designed and synthesized for utilization in a chemoproteomics pull-down assay as an unbiased approach for identifying potential *E. faecium* protein targets (Scheme S1). The AZM-based pull-down probe Biotin-AZM consists of an AZM scaffold tethered to biotin via a PEG_8 linker. As a negative control based on prior structure−activity relationships, pull-down probe, Biotin-Neg was designed in the same manner, except with the sulfonamide replaced by a methyl sulfone group. The sulfone analog does not inhibit the bacterial CAs[30] nor exhibit any antimicrobial activity[29] likely through the loss of coordination to the Zn^{2+} in the CA active site. We confirmed the Biotin-AZM probe maintained in vitro inhibition of both the α- and γ-CAs with K_i values of 66 and 204 nM, respectively. Conversely, the Biotin-Neg probe did not inhibit either bacterial CA at concentrations up to 10 μM. We also tested both probes for antibacterial activity against *E. faecium* in MIC assays, but they did not maintain activity up to 64 μg/mL, which may be due to large changes in the lipophilicity and molecular weight of the probe for whole-cell activity. Thus, we performed the pull-downs on lysates to remove the molecule entry variable.

The native expression level of each bacterial CA was quantified to understand relative expression using global label-free quantification (LFQ) proteomics. For this, we grew *E. faecium* in overnight cultures, pelleted, washed, and lysed the cells in biological triplicate. Lysates were normalized to total protein concentration, then prepared for bottom-up proteomics with trypsin digestion followed by LC-MS/MS analysis. The LFQ intensities were normalized to protein concentration in each sample. The data showed that the α-CA isoform has significantly greater expression, 2.1×10^7 normalized LFQ intensity, compared to the γ-CA with 4.0×10^5 normalized LFQ intensity (Figure S1).

These biotin-functionalized probes were then employed in a pull-down assay with magnetic streptavidin beads to enrich target proteins from *E. faecium* lysates. Baseline control samples were prepared in which streptavidin beads were treated with DMSO rather than the probe to evaluate nonspecific protein binding to the beads. The lysates (biological triplicate) were then incubated with probe-treated and DMSO-treated streptavidin beads, followed by washing with PBS, and gentle elution of weak binders. The beads were prepared for a bottom-up proteomics sample with on-bead trypsin digestion, followed by LC-MS/MS analysis. Peptides detected were matched to their corresponding proteins to identify targets and were quantified based on normalized abundances. Both Biotin-AZM and Biotin-Neg datasets were compared to the DMSO control datasdaet to account for nonspecific binders to streptavidin.

Overall, 806 total proteins were identified across all three treatment groups (full dataset provided in Supporting Information), and the data were visualized in volcano plots based on the $\log_2$(fold-change) in protein abundance and on the $-\log_{10}$(p-value) for statistical significance, between probe-treated and DMSO-treated lysates (Figure 2). Proteins

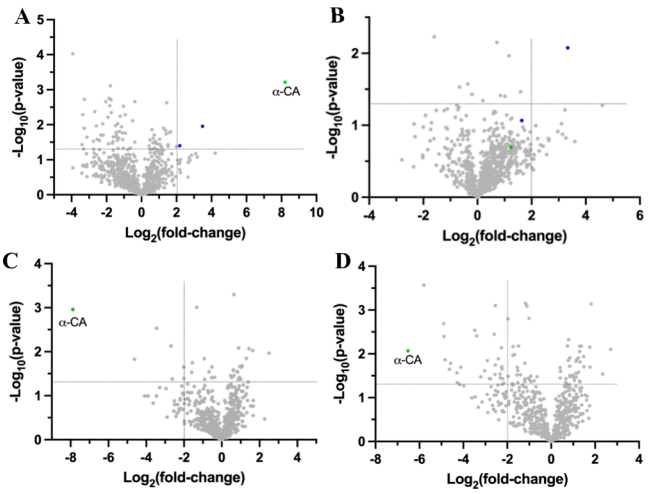

Figure 2. Chemoproteomics pull-down assay volcano plots from *E. faecium* lysates. (A) Protein enrichment in Biotin-AZM pull-down samples compared to DMSO control pull-down samples. (B) Protein enrichment in Biotin-Neg pull-down samples compared to DMSO control pull-down samples. Criteria for enriched proteins ($-\log_{10}$(p-value) $\geq$ 1.3; $\log_2$(fold-change) $\geq$ 2) are depicted by dashed lines. *E. faecium* α-CA is dlabeled as a green circle. Other proteins found to be enriched by Biotin-AZM are indicated as blue circles. (C) AZM preincubation compared to the Biotin-AZM probe. (D) CAI0019 preincubation compared to the Biotin-AZM probe. Criteria for competed off proteins ($-\log_{10}$(p-value) $\geq$ 1.3; $\log_2$(fold-change) $\leq$ −2) are depicted by dashed lines. *E. faecium* α-CA is labeled as a green circle in all panels.

enriched by a $\log_2$(fold-change) of ≥2.0 and $-\log_{10}$(p-value) of ≥ 1.3 were considered statistically significantly enriched by 4-fold or more in the Biotin-AZM pull-down compared to the DMSO control pull-down. A total of three protein candidates met these criteria (Figure 2, Table 2), with the *E. faecium* α-CA showing the greatest enrichment in the Biotin-AZM pull-down with 8.21 $\log_2$(fold-change) with a 3.22 $-\log_{10}$(p-value). The two additional proteins enriched by Biotin-AZM included L-lactate oxidase and a homocysteine-S-methyltransferase protein. Neither the *E. faecium* α-CA nor homocysteine S-methyltransferase was enriched on the Biotin-Neg negative control probe, indicating these may bind specifically to the Biotin-AZM (Figure 2B, Table 2). Conversely, L-lactate oxidase was significantly enriched on the negative control Biotin-Neg (Figure 2, Table 2), suggesting this may bind the probe or AZM scaffold independently of the sulfonamide and is likely not relevant for biological effect. Interestingly, *E. faecium* γ-CA was not identified in any of the samples despite

https://doi.org/10.1021/acsinfecdis.5c00736
ACS Infect. Dis. 2026, 12, 176−189

Table 2. Annotated Proteins Enriched Pull-Down Assay by Biotin-AZM and Biotin-Neg Probes Compared to DMSO Controls in Pull-Down Assay

		(Biotin-AZM) − DMSO[a]		(Biotin-Neg) − DMSO[b]		AZM − (Biotin-AZM)		CAI0019 − (Biotin-AZM)	
acc #[c]	description	$-\log_{10}$ (p-value)	$\log_2$ (FC)[d]	$-\log_{10}$ (p-value)	$\log_2$ (FC)[d]	$-\log_{10}$ (p-value)	$\log_2$ (FC)[d]	$-\log_{10}$ (p-value)	$\log_2$ (FC)[d]
Q3XYE8	α-carbonic anhydrase	3.22	8.21	0.69	1.24	2.96	−7.88	2.07	−6.52
Q3Y1Q6	L-lactate oxidase	1.96	3.49	2.08	3.33	n.d.[e]	n.d.[e]	n.d.[e]	n.d.[e]
Q3Y1Z7	homocysteine S-methyltransferase	1.40	2.19	1.07	1.64	0.06	0.15	0.02	−0.04

[a]Normalized protein abundance detected in the DMSO-treated sample was subtracted from the Biotin-AZM probe samples. [b]Normalized protein abundance detected in the DMSO-treated sample was subtracted from the Biotin-Neg probe samples. [c]Uniprot protein accession number corresponding to the samples. [d]FC = fold-change. [e]n.d. = not determined, lack of detection in competition assay.

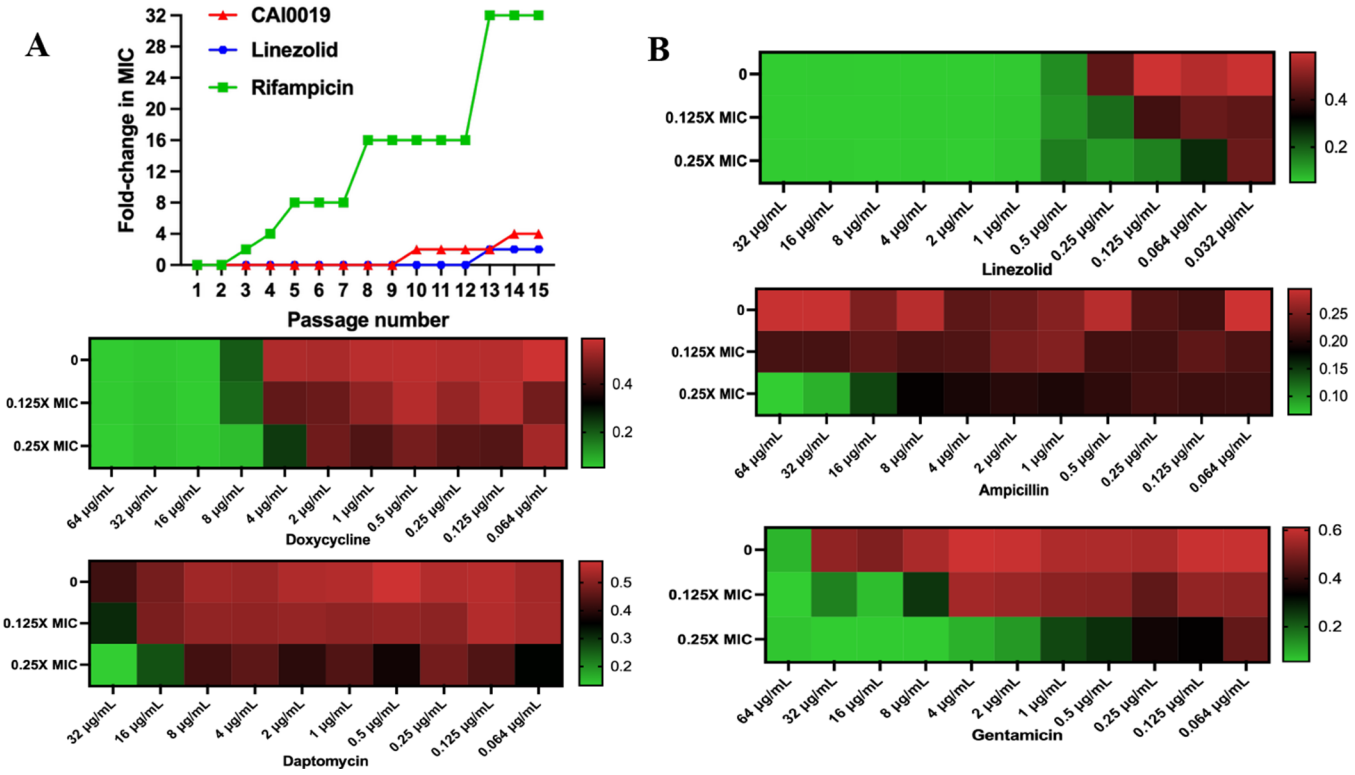

Figure 3. Preclinical antimicrobial evaluation for CAI0019. (A) Multistep resistance selection of CAI0019 against the VR *E. faecium* NR-31909. Bacteria were serially passaged with test agents for 15 days, and the broth microdilution assay was used to determine the MICs for CAI0019, linezolid, and rifampicin against VRE after each successive passage. (B) Combination testing of CAI0019 with different antibiotics against the VR *E. faecium* NR-31909. CAI0019 was tested at 0.125 and 0.25 × MIC in combination with either linezolid, daptomycin, ampicillin, gentamycin, or doxycycline against *E. faecium* NR-31909, and the FIC values were calculated. Interactions where the FICI was ≤0.5 were categorized as synergistic, an FICI value of >0.5 to 1.25 was considered additive, an FICI value of >1.25 to 4 was considered indifferent, and FICI values of >4 were considered antagonistic. Scale bars represent OD_{600} reading, n = 3 biological replicates for both MPC and synergy testing.

the AZM inhibiting the enzyme with a K_i value of 323 nM. The lack of enrichment on pull-down may be attributed to the significantly greater expression of the α-CA isoform in the bacterial cells. The α-CA isoform, with a greater affinity and expression level 2 orders of magnitude greater than the γ-CA, may simply be able to outcompete for the limited Biotin-AZM probes on beads. Therefore, these data do not rule out the γ-CA as a secondary target but indicate a low probability of being a primary target for the scaffold.

To further investigate *E. faecium* α-CA engagement of AZM and CAI0019, competition pull-down experiments were performed in which lysates were preincubated with 100 μM of free inhibitor AZM or CAI0019 prior to the pull-down to compete with Biotin-AZM for target binding. Criteria determining the proteins that successfully competed off from the pull-down probe by inhibitors were defined as proteins with a $\log_2$(fold-change) less than −2 and a $-\log_{10}$(p-value) greater than 1.3.

The results from the pull-down competition experiments indicated that AZM and CAI0019 both significantly compete off the α-CA from the Biotin-AZM probe, as shown by the strong negative $\log_2$(fold-change) in α-CA enrichment on the beads when compared to that of the standard Biotin-AZM pull-down using *E. faecium* lysates pretreated only with DMSO (Figure 2, Table 2). L-lactate oxidase was not detected in the competition samples, and 5-methyltetrahydropteroyltriglutamate-homocysteine S-methyltransferase was not negatively enriched in the competition datasets, further strengthening the conclusion that these proteins were likely false positives that lack biological relevance to the antimicrobial effect of the

https://doi.org/10.1021/acsinfecdis.5c00736
ACS Infect. Dis. 2026, 12, 176−189

inhibitors themselves. The results taken together with the fact that *Enterococcus* species are no longer susceptible to AZM or CAI0019 in 5% CO_2 all strongly indicate that the α-CA is the primary target for antimicrobial activity for the scaffold. The full datasets are provided in the Supporting Information.

Preclinical Antimicrobial Evaluation for CAI0019. CAI0019 was previously shown to exhibit bacteriostatic antienterococcal activity.[29] To further investigate the potential for translation of CAI0019, we evaluated the molecule in several preclinical antimicrobial assays, including resistance, postantibiotic effect (PAE), and drug synergy screening. First, we examined the potential to develop resistance to CAI0019 using a multistep resistance selection assay against the *E. faecium* NR-31909 clinical strain. The MIC of CAI0019 increased by only 2-fold MIC at passage 10 and by 4-fold MIC on passage 14, indicating that *E. faecium* did not develop significant resistance to CAI0019 (Figure 3). This trend was comparable to what was observed for linezolid, which showed a 2-fold MIC increase in MICs starting at passage 13. In contrast, *E. faecium* rapidly acquired resistance to rifampicin, with an 8-fold MIC increase after just five passages, followed by a gradual rise throughout the experiment. These results indicate a slight drift in MIC after multiple passages but do not indicate significant resistance development over the course of the assay.

Next, we evaluated the PAE, the period after complete removal of the drug in which an antibiotic effect is still observed. The PAE was determined for CAI0019 and linezolid against two VRE strains. Linezolid and CAI0019 displayed an observed PAE ranging from 1 to 2 h against the two strains tested (Table S1). These results are consistent with previous reports, which showed that linezolid's PAE are within the same range for different Gram-positive bacteria, including staphylococci and enterococci.[54] The short PAE of CAI0019 could be attributed to its bacteriostatic activity against the VRE.

Finally, using the standard checkerboard assay, we investigated the interactions of CAI0019 with different antibiotics currently or previously used to combat VRE infections using different mechanisms of action. CAI0019 exhibited a synergistic interaction with ampicillin and gentamicin against the tested strain, with a fractional inhibitory concentration index (FICI) of $\leq$0.5 and 0.28, respectively (Figure 3). Alternatively, CAI0019 demonstrated an additive relationship with linezolid, daptomycin, and doxycycline against the tested strain. The synergy with gentamicin is an observation that has previously been noted in the *E. faecalis* strain that was isolated from an endocarditis patient that had a single-point mutation resulting in a stop codon placed in the middle of the α-CA gene, yielding an inactive enzyme.[55] This particular strain was susceptible to gentamicin due to increased proton motive force-powered uptake and increased membrane permeability.

In Vitro ADME Properties for CAI0019. Next, we evaluated CAI0019 for in vitro ADME and physicochemical properties related to drug-likeness (Table 3). Our prior reports on CAI0019 note log $D_{7.4}$, solubility in PBS (pH 7.4), and Caco-2 permeability[29,40] and we have relisted those values here for full evaluation of in vitro ADME. Orally effective drugs typically reside within chemical space MW < 500 Da and log $D_{7.4}$ values ranging from 1 to 3,[56] which is where CAI0019 resides with a MW = 318.4 Da and log $D_{7.4}$ = 2.26. Solubility is around 30 μM in both PBS at pH 7.4 and simulated intestinal fluid at pH 6.5; thus, the molecule has an upper solubility limit

Table 3. In Vitro ADME Profile for CAI0019

MW		318.4
log $D_{7.4}$		2.26[a]
solubility (μM)	PBS, pH 7.4[b]	33.0[a]
	SIF, pH 6.5[c]	30.2
	SGF, pH 1.2[d]	25.0
Caco-2P_{app} (10^{-6} cm/s)[e]	A → B (% rec)[f]	6.5 (35%)[a]
	B → A (% rec)[f]	14.1 (53%)[a]
mouse plasma f_u[g]		0.06
mouse liver microsome stability[h]	% @ 15 min	87.3
	30	79.0
	45	68.8
	60	51.8
	$t_{1/2}$ (min)[i]	66.9
	Cl_{int} (μL/min/mg)[j]	103.6

[a]Previously reported by Kaur et al.[29] and Abutaleb et al.[40] [b]PBS = phosphate-buffered saline. [c]SIF = simulated intestinal fluid. [d]SGF = simulated gastric fluid. [e]P_{app} = apparent permeability coefficient. A = apical, B = basolateral. pH 6.5/7.4 in receiver/donor chambers. [f]% rec = % recovery from media after assay. [g]f_u = fraction unbound. [h]% remaining at each time point. [i]$t_{1/2}$ = half-life. [j]Cl_{int} = intrinsic clearance.

in aqueous media that is 21- to 173-fold the MIC levels for the molecule. Bidirectional Caco-2 apparent permeability (P_{app}) was evaluated as an estimate of intestinal absorption. CAI0019 demonstrated moderate P_{app} values in both apical-to-basolateral (6.5×10^{-6} cm/s) and in the reverse direction (14.1×10^{-6} cm/s), which suggests the molecule would likely have high oral bioavailability with slight efflux potential in vivo. One caveat to the Caco-2 results is that the molecule displayed approximately 50% or lower percent recovery in the assay, possibly due to nonspecific binding to cells and lysosomal sequestration[57] and/or potential intracellular binding to endogenous human CA expressed in Caco-2 cells, such as CA XIII, leading to sequestration within the cells. The molecule exhibited high mouse plasma protein binding with a fraction unbound (f_u) of 0.06, similar to that of AZM. Finally, CAI0019 was evaluated for stability in mouse liver microsomes as a surrogate to estimate metabolism for the molecule and found to be 51.8% remaining after 60 min incubation, resulting in a half-life of 66.9 min and intrinsic clearance of 103.6 μL/min/mg. These values indicate that CAI0019 may be prone to phase 1 oxidative metabolism. In summary, despite high plasma protein binding and potential for metabolic liability, the molecule possesses favorable physicochemical properties and ADME values to be considered a candidate for oral treatment of *E. faecium* infection.

In Vivo Pharmacokinetics for CAI0019 in Mice. CAI0019 was next evaluated for in vivo pharmacokinetics (PK) in mice. In our prior report on the development of CAI0019, we demonstrated that the molecule is orally bioavailable with in vivo plasma values in mice after a 10 mg/kg *per os* (PO) dose.[29] Our current study was designed to assess standard PK metrics, including quantification of oral bioavailability, but also blood partitioning for the molecule. It is well established that CA inhibitors, as demonstrated with AZM, partition into the red blood cell (RBC) portion of the blood over the plasma due to expression of both human CA 1 and 2 within the erythrocyte.[58] Thus, we evaluated CAI0019 concentration in whole blood after both intravenous (IV) doses at 5 mg/kg and *per os* (PO) doses at 10 mg/kg to determine oral bioavailability. We also compared the prior

https://doi.org/10.1021/acsinfecdis.5c00736
ACS Infect. Dis. 2026, 12, 176−189

reported CAI0019 plasma concentration after a 10 mg/kg PO dose to determine blood partitioning (Figure 4 and Table 4, tabular data in Tables S2−S5).

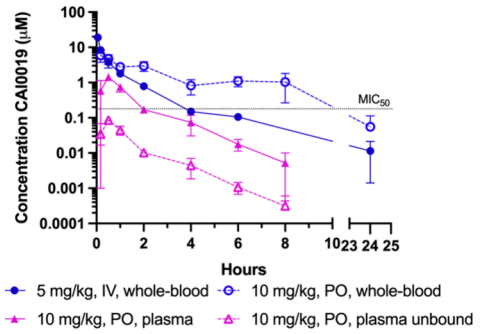

Figure 4. In vivo pharmacokinetic analysis of CAI0019 in mice. Concentration curves are shown for whole blood after a 5 mg/kg IV dose (blue circles) and a 10 mg/kg PO dose (blue open circles). Concentration curve for plasma (magenta triangles, reported by Kaur et al.[29]) and $plasma_u$ (open magenta triangles) after a 10 mg/kg PO dose is shown. All data points are mean ± standard deviation for each time point (n = 3 per time point). Concentration for MIC_{50} depicted by a black dotted line.

Table 4. In Vivo Pharmacokinetic Metrics for CAI0019 in Mice[a]

	whole blood		plasma[b]	$plasma_u$[c]
	5 mg/kg IV	10 mg/kg PO	10 mg/kg PO	10 mg/kg PO
C_{max} (μM)[d]	29.33	5.94	1.43	0.086
$AUC_{0\to 24h}$(h*μM)[e]	19.32	23.67	1.76	0.11
F (%)[f]		61.8		

[a]Values are determined from n = 3 mice per time point. [b]Reported by Kaur et al.[29] [c]$Plasma_u$ was determined using the fraction unbound for CAI0019 of 0.06 in mouse plasma. [d]Maximum concentration of CAI0019 measured in each medium. [e]Area under the curve for CAI0019 in each medium over the time course of the experiment. [f]Oral bioavailability determined from whole-blood samples.

The data showed that CAI0019 is rapidly absorbed after oral dose with a maximum concentration (C_{max}) of 5.94 μM in whole blood observed at the 10-min time point. In the plasma fraction, C_{max} of 1.43 μM was reached later at the 30-min time point. The area under the curve over 24 h (AUC_{0-24h}) exposure of CAI0019 in whole blood after both 5 mg/kg IV and 10 mg/kg PO dosing routes of administration was shown to be 19.32 and 23.67 h*μM, respectively. When normalized according to dose, oral bioavailability (F) was determined to be 61.8% for the molecule. The AUC_{0-24h} in plasma at the 10 mg/kg PO dose was 1.76 h*μM, amounting to a 13.4-fold decrease from the whole blood AUC_{0-24h}, suggesting high blood partitioning into RBCs. Evidence for blood partitioning of the AZM scaffold was initially reported by Wallace et al. after observing that AZM exhibits 4-fold partitioning into RBCs over plasma in healthy human subjects.[59] The increased blood partitioning for CAI0019 may be partially attributed to the almost 40-fold increased potency for human CA 2 inhibition for CAI0019 compared to that of AZM (Figure 1). Although mouse RBCs contain murine CA 2 (mCA 2)[60,61] rather than hCA 2, the mCA 2 (UniProt ID: P00920) is highly homologous to hCA 2 (UniProt ID: P00918) with which it shares 81% sequence identity and 93% similarity (Figure S2), suggesting that our AZM-based inhibitors would similarly engage mCA 2.[62] Finally, the plasma unbound fraction ($plasma_u$) was determined using the mouse plasma f_u value of 0.06. Adjusting for $plasma_u$ at the 10 mg/kg PO dose drops the maximum exposure below that of the MIC_{50} for CAI0019 against *E. faecium* and *E. faecalis* strains, suggesting the need for a larger dose size to achieve $plasma_u$ exposure high enough to demonstrate efficacy in vivo.

Efficacy of CAI0019 in a Mouse Model for *E. faecium* Septicemic Peritonitis. Following PK characterization, CAI0019 was carried forward for evaluation in an *E. faecium* septicemic peritonitis mouse model. Due to the 10 mg/kg PO *quaque die* (QD) dose demonstrating exposure below the MIC_{50} for the plasma unbound fraction, our team chose to dose CAI0019 for the proof-of-concept study at 20 mg/kg PO, QD for 3 days. Eight-week-old BALB/c mice were infected intraperitoneally with *E. faecium* NR-31909 suspension containing 5% mucin at an inoculum of 5.43×10^7 CFU/mL. One hour later, groups were randomly chosen (n = 6/group), and mice were treated with 20 mg/kg PO of either CAI0019, AZM (treatment group), or linezolid (positive control group) while a fourth group was treated with vehicle (negative control group). Mice received treatments once daily for 3 days before they either succumbed to the infection or were humanely euthanized at the end of the study. In the study, both CAI0019 and linezolid rescued 83% (5 out of 6 mice), followed by AZM rescuing 66.7% (4 out of 6 mice) (Figure 5). These numbers were significant improvements over the vehicle-treated cohort, which only saw 16.7% survival (1 out of 6 mice).

To determine the effect of the molecule on VRE bioburden after treatment, the *E. faecium* burden in organs was quantified from each mouse in each cohort (Figure 5 and Table S6). Across the kidney, liver, and spleen tissues, the treatments AZM and CAI0019 were equally as efficacious as linezolid. All displayed agf significant reduction with at least a 2-log_{10} CFU/mL reduction of VRE bioburden compared to the vehicle-treated control in each tissue. These values are equivalent to >99% reduction of VRE bioburden over the 3-day treatment. These results corroborate the efficacy of rescuing mice in the same model.

Effect of CAI0019 on Mouse Microbiome Diversity. With the promising proof-of-concept results for CAI0019 in the *E. faecium* septicemic peritonitis model, we were motivated to evaluate the molecule for its effect on mouse microbiome diversity. Microbiome dysbiosis in the GIT is a contributor to numerous other adverse health conditions. Thus, the development of therapeutics capable of selectively eliminating VRE infection while sparing the GIT microbiota would be preferred. As mentioned, bicarbonate is a critical metabolic building block to support bacterial growth. Bacteria typically rely on one of two mechanisms to satisfy bicarbonate needs for growth: DIC transporters or CAs. *E. faecium* and *E. faecalis* are among several pathogens that do not encode for *mpsAB* DIC genes but do encode for CAs.[48] It is our hypothesis that due to the CA inhibition mechanism of action, CAI0019 will spare the microbiome, as these bacteria will be able to supplement bicarbonate via MpsA and MpsB homologues. Thus, to test our hypothesis, we carried out an in vivo experiment to assess alterations in the GIT microbiome diversity before, during, and after 14-day treatment with CAI0019.

For this experiment, C57BL/6 mice (n = 5/group) were treated with CAI0019 (20 mg/kg, PO QD for 14 days),

https://doi.org/10.1021/acsinfecdis.5c00736
ACS Infect. Dis. 2026, 12, 176−189

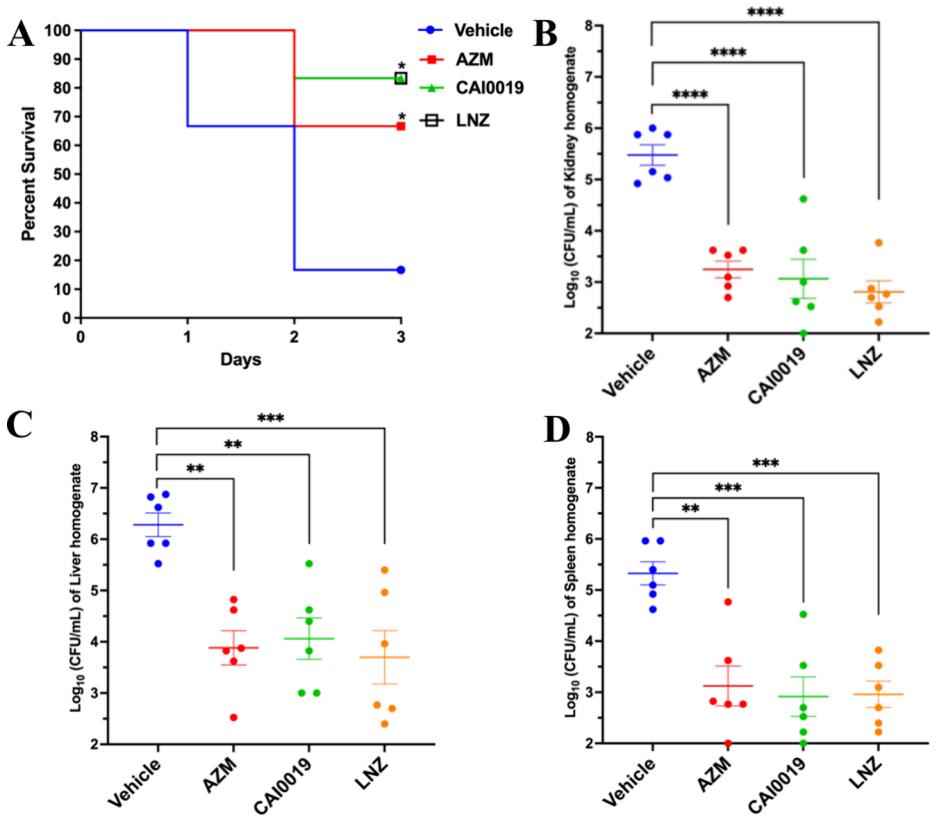

Figure 5. In vivo efficacy of CAI0019 and AZM in murine VRE peritonitis model after infection with *E. faecium* NR-31909. (A) Kaplan−Meier survival curves were analyzed using the log-rank (Mantel-Cox) test. The asterisk (*) denotes a statistically significant difference ($p < 0.05$) in comparison between treated mice and vehicle-treated mice ($n = 6$/group). Organ tissue from the kidneys (B), liver (C), and spleen (D) of infected mice was collected at the time of death for vehicle-treated mice and at day 3 for all surviving animals. The CFU/mL data were analyzed via a one-way ANOVA with *post hoc* Dunnett's test for multiple comparisons. Asterisks denote significant differences for treatment groups compared to the vehicle group ($n = 6$/group). ** indicates $p < 0.01$, *** indicates $p < 0.001$, **** indicates $p < 0.0001$.

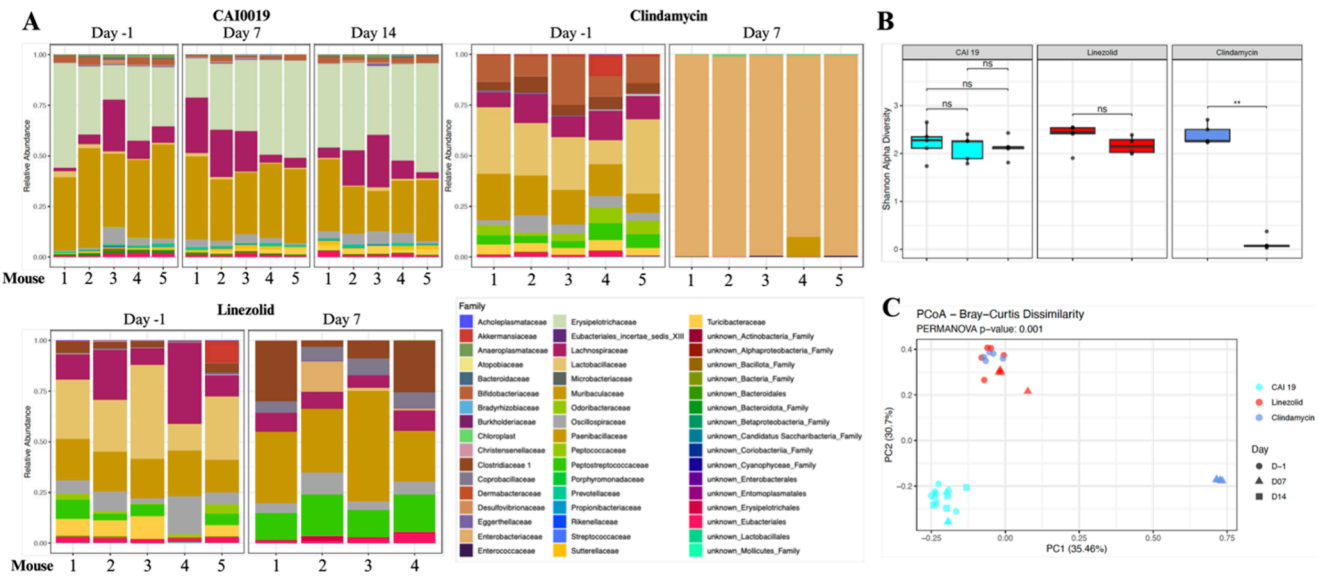

Figure 6. Mouse gut microbiome diversity in fecal pellets upon antibiotic treatments. (A) Taxonomic analysis at the family level showing bacterial population changes after oral antibiotic administration from day −1 (predose) to day 7 (all groups) and day 14 (for CAI0019). (B) Shannon alpha diversity index analysis of each cohort comparing pre- and postdose microbiome diversity ($n = 5$ mice per group except for linezolid day 7 samples ($n = 4$)). Unpaired Wilcoxon rank-sum tests with *p*-values (adjusted for multiple comparisons using the Benjamini−Hochberg method) comparing the differences in Shannon Alpha Diversity between predose samples and postdose samples. Boxes span the first to the third quartiles, center lines represent median values, and whiskers show data points within 1.5× the interquartile range of the top and bottom quartiles. ** p (adjusted) < 0.01, ns = not significant. (C) Beta diversity assessed by Bray−Curtis dissimilarity from untransformed 16S rRNA gene count data.

https://doi.org/10.1021/acsinfecdis.5c00736
ACS Infect. Dis. 2026, 12, 176−189

linezolid (20 mg/kg PO QD for 7 days), or clindamycin (positive control, 100 mg/kg PO QD for 7 days). Fecal samples were collected at day −1 prior to treatment to serve as a negative control for the changes in microbiome diversity within the same mouse after treatments. Fecal samples were aseptically collected at day 7 for all groups and at day 14 for the CAI0019 group. DNA was extracted from fecal samples and submitted for microbiome metagenomics analysis of the V4−V5 region of 16S RNA (rRNA) sequencing and qPCR quantification to provide relative abundance values (Figure 6). It should be noted that a complication arose during initial dosing of linezolid in one mouse, resulting in the animal being sacrificed without collecting any postdose fecal sample pellets; therefore, the cohort size for linezolid day 7 is 4. Additionally, mice for the clindamycin and linezolid control groups were ordered separately and cohoused together prior to ordering the mice for the CAI0019 test group. This accounts for an initial difference in the day −1 microbiomes between the control groups and CAI0019 groups. However, since the study is to evaluate changes in diversity within each cohort, the day −1 predose controls for each group are valid for comparison to postdose time points.

CAI0019-treated mice exhibited no significant changes in microbiome diversity in the fecal samples at days 7 or 14 compared to the fecal pellets collected prior to treatment. This is reflected by the lack of a statistically significant change in the Shannon Alpha Diversity and beta diversity values for pre- and post-treatment fecal samples. These results indicate that the microbiomes of the CAI0019 treatment groups maintained sufficient species richness and diversity throughout the prolonged treatment regimen. Additionally, the mice generally tolerated the prolonged 20 mg/kg PO QD treatment with CAI0019 and did not exhibit any deleterious effects on animal health or well-being when observed and scored during treatment. An illustration of the tolerability for the molecule can be observed in the lack of significant body weight loss over the 14 days of treatment for the mice (Figure S3). Interestingly, the linezolid cohort also exhibited no significant change in microbiome diversity when comparing the pretreatment to the day 7 fecal samples, even though the molecule is active in vitro against microbiome bacteria and demonstrated mouse gut dysbiosis in other studies when dosed at 100 mg/kg PO.[10] This is a lack of effect from linezolid is likely attributable to the rapid intestinal absorption of linezolid[63] and the lower dose of 20 mg/kg compared to prior studies, resulting in a low concentration of the molecule retained in the GIT.[64]

DISCUSSION

The results of this study confirm the intracellular target for the 1,3,4-thiadiazole class of antienterococcal agents to be the bacterial α-CA and provide in vivo data demonstrating efficacy in a mouse model for septicemic peritonitis while having no significant effect on the GIT microbiome diversity. These findings are an extension of previous work by our team in hit-to-lead optimization of the scaffold to improve antibacterial properties against VRE and demonstrate efficacy in decolonization of *E. faecium* from mouse GITs. While prior studies demonstrated antimicrobial activity for the scaffold, questions remained regarding both the intracellular target and the mechanisms that elicit the antimicrobial effect against the pathogen. This study is the first to confirm target engagement with α-CA. Interestingly, the results indicate that γ-CA is likely not an intracellular target for the scaffold. Indeed, based on K_i alone, AZM and CAI0019 are >5-fold more potent against the α-CA over the γ-CA, and this is to be expected as the scaffold was originally designed for closely related human α-CAs. Moreover, follow-up genetic studies, such as knockdown or complementation of the CA genes to further validate the chemoproteomics results, were unsuccessful. Notably, *E. faecium* is known to be difficult to study using genetic approaches due to underlying DNA defense mechanisms that prevent foreign DNA-plasmids from effectively entering the cell.[65,66] Thus, even without genetic validation, we believe the data in its totality point to a high probability that α-CA inhibition is the primary means for antibacterial activity.

With the scaffold confirmed to be targeting the α-CA, there are still questions as to how inhibiting the CA mediates an antibacterial response. Prior literature investigates the role of bicarbonate in central carbon metabolism for bacteria, demonstrating that bicarbonate serves as a critical carbon source to support bacterial growth, including anaplerotic reactions involving biotin-dependent carboxylation[67] to supply components of central metabolism with oxaloacetate[42] and acetyl-CoA.[43,68] Acetyl-CoA is also the substrate for the first committed step in fatty acid biosynthesis, as it is converted into malonyl-CoA by acetyl-CoA carboxylase, again using bicarbonate.[43,68] Moreover, bicarbonate has been shown to be critical for de novo purine biosynthesis in bacteria[45] as it is a substrate for PurK, the enzyme that carries out an irreversible step of converting aminoimidazole ribonucleotide to carboxyaminoimidazole ribonucleotide.[69] Investigations in *E. coli* have shown that there is a high metabolic need for bicarbonate to support central carbon flux and that dropping below that threshold renders the bacteria unable to sustain growth.[46] These prior studies suggest that the antibacterial properties of the bacterial CA inhibitors could be attributed to the disruption of these bicarbonate-dependent pathways. Additionally, there is the possibility that residual γ-CA activity in the cell could compensate for the loss of α-CA activity. Future work to design inhibitors with more potent γ-CA activity could provide additional improvements in antibacterial activity.

More recent findings describe DICs, i.e., bicarbonate transporters, as a primary means to satisfy the bicarbonate needs of a widespread array of bacteria. Within these reports, the authors demonstrate that most bacteria rely on DICs; however, a relatively small number of bacterial pathogens lack DICs and require CAs to meet the bicarbonate needs. Among these were *Enterococcus* species.[48] Additionally, in follow-up studies, the same group demonstrated that if bacteria have both DICs and CA encoded, the fitness of the species is reliant on the DIC activity.[49] Thus, based on this literature, we tested CAI0019 and AZM against *B.* subtilis that encodes both CA and *mpsAB* genes, and the molecules were not active. These studies suggest that CA inhibitors may occupy a unique niche of narrow-spectrum activity that may allow the class to have no significant effect on the GIT microbiome diversity. We tested the hypothesis by conducting an in vivo mouse microbiome diversity experiment and demonstrated no significant change in GIT microbiome diversity after prolonged daily oral treatment of CAI0019 at an efficacious dose of 20 mg/kg. Taken together, these results further validate bacterial CA inhibition as a viable antibiotic therapeutic strategy, provide a mechanistic underpinning to the observed antimicrobial effect, and suggest that CAs may be uniquely positioned as an antibiotic target while sparing the GIT microbiome.

https://doi.org/10.1021/acsinfecdis.5c00736
ACS Infect. Dis. 2026, 12, 176−189

The results reported herein also provide rationale to evaluate CA inhibition in a variety of other pathogens that lack DICs but encode CA genes (similar to those of *Enterococcus*). Among these are high-priority pathogens such as *Mycobacterium tuberculosis*, *Helicobacter pylori*, *Pseudomonas aeruginosa*, *E. coli*, and *N. gonorrheae*.[46,48,70] Prior work has already been reported investigating CA inhibition against *M. tuberculosis*[71] and *H. pylori*[72,73]; however, these studies were not focused on translation to animal models. Additionally, a recent report suggests *A. baumannii* may be susceptible to CA inhibition in certain conditions, but requires efflux pump knockout to gain intracellular access to the CA.[74] Our studies demonstrated that bacterial CA inhibition can lead to efficacious in vivo activity and afford the opportunity to test the hypothesis that CA inhibition would be a viable approach to target additional high-priority pathogens.

While the sum of the study demonstrates on-target α-CA inhibition is a viable antienterococcal therapeutic strategy able to spare the microbiome, there remain limitations, particularly for CAI0019 as a lead compound. The main limitation is with respect to the inhibition of human CAs. While AZM can be dosed at over 1 g/day in humans with few adverse effects,[75] CAI0019 is more potent against hCA 2, which may reduce its tolerability. Aside from blood partitioning data, we do not yet know the consequences of CAI0019 mammalian CA inhibition in vivo, particularly with respect to whether the molecule maintains a diuretic effect and what the maximum tolerated dose may be. Additionally, it remains unclear as to the effect mammalian CA binding may have on the distribution of the molecule to tissues relevant for infection and the overall effect on reducing enterococcal bioburden. However, this provides an opportunity for future analog design to be directed toward increasing selectivity over hCAs while maintaining antienterococcal activity. If this can be achieved, such molecules may demonstrate improved plasma unbound exposure while widening the therapeutic window, in turn allowing for more pharmacokinetic/pharmacodynamic evaluation of the scaffold. This would represent a critical advancement toward ultimately fulfilling the therapeutic potential for the class and could subsequently provide motivation toward exploring the potential of targeting CAs in other bacterial pathogens mentioned above.

The results of this study fill a scientific gap and expand on the benefits of bacterial CA inhibition as a viable antibiotic approach. Utilizing a chemoproteomic approach with an AZM-based biotin probe, our team identified the *E. faecium* α-CA as the primary binding target for the 1,3,4-thiadiazole-sulfonamide scaffold. The lead molecule CAI0019 demonstrates potent antienterococcal activity with efficacy in rescuing mice in a lethal septicemic peritonitis model of *E. faecium* infection after oral dosing. Finally, we hypothesized based on the mechanism of action that bacterial CA inhibitors would represent narrow-spectrum agents capable of sparing the GIT microbiome. This hypothesis was supported by data demonstrating that mice treated daily with oral doses of CAI0019 had no significant alterations in microbiome diversity. The summation of these studies supports the potential for translating bacterial CA inhibitors for the treatment of *E. faecium* and could ultimately open the door for CA inhibition in combating other drug-resistant bacteria.

MATERIALS AND METHODS

Chemistry General Information. CAI0019 was obtained as previously described.[29] All synthetic methods for obtaining chemoproteomics probes Biotin-AZM and Biotin-Neg are provided in the Supporting Information.

Biological General Information. Materials and methods for biological evaluation are provided in the Supporting Information.

ASSOCIATED CONTENT

Data Availability Statement

Proteomics data have been deposited in MassIVE repository under the id MSV000098878 and MSV000099801.

Supporting Information

The Supporting Information is available free of charge at https://pubs.acs.org/doi/10.1021/acsinfecdis.5c00736.

Native expression LFQ CA intensities, synthetic scheme for chemoproteomics probes, whole blood and plasma concentrations in mice from intravenous and oral dosing, unbound plasma concentrations in mice after oral dosing, *E. faecium* tissue bioburden values, Uniprot sequence alignment for mCA2 and hCA2, mouse body weight over 14-day dosing with CAI0019, synthetic protocols for Biotin-AZM and Biotin-Neg, compound characterization including ^{1}H- and ^{13}C NMR spectra and mass spectra for pull-down probes, materials, and methods are provided (PDF)

Chemoproteomic native expression and pull-down data provided in XLSX. Microbiome Taxonomy Classification per mouse provided in XLSX. (XLSX)

Pull-downBiotin-AZM probe data (XLSX)

Pull-downcompetition data (XLSX)

Globalproteomic levels (XLSX)

AUTHOR INFORMATION

Corresponding Authors

Mohamed N. Seleem − *Department of Biomedical Sciences and Pathobiology, Virginia-Maryland College of Veterinary Medicine, Virginia Polytechnic Institute and State University, Blacksburg, Virginia 24061, United States; Center for One Health Research, Virginia Polytechnic Institute and State University, Blacksburg, Virginia 24061, United States;* orcid.org/0000-0003-0939-0458; Email: seleem@vt.edu

Daniel P. Flaherty − *Borch Department of Medicinal Chemistry and Molecular Pharmacology, College of Pharmacy, Purdue University, West Lafayette, Indiana 47907, United States; Purdue Institute for Drug Discovery, West Lafayette, Indiana 47907, United States; Purdue Institute of Inflammation, Immunology and Infectious Disease, West Lafayette, Indiana 47907, United States;* orcid.org/0000-0002-8305-0606; Email: dflaher@purdue.edu

Authors

Nader S. Abutaleb − *Department of Biomedical Sciences and Pathobiology, Virginia-Maryland College of Veterinary Medicine, Virginia Polytechnic Institute and State University, Blacksburg, Virginia 24061, United States; Center for One Health Research, Virginia Polytechnic Institute and State University, Blacksburg, Virginia 24061, United States*

Katrina J. Holly − *Borch Department of Medicinal Chemistry and Molecular Pharmacology, College of Pharmacy, Purdue University, West Lafayette, Indiana 47907, United States*
Carolyn K. Metcalfe − *Borch Department of Medicinal Chemistry and Molecular Pharmacology, College of Pharmacy, Purdue University, West Lafayette, Indiana 47907, United States;* orcid.org/0000-0002-9304-8681
Ahmed A. Abouelkhair − *Department of Biomedical Sciences and Pathobiology, Virginia-Maryland College of Veterinary Medicine, Virginia Polytechnic Institute and State University, Blacksburg, Virginia 24061, United States; Center for One Health Research, Virginia Polytechnic Institute and State University, Blacksburg, Virginia 24061, United States;* orcid.org/0000-0001-9937-742X
Prabhakara R. Tharra − *Borch Department of Medicinal Chemistry and Molecular Pharmacology, College of Pharmacy, Purdue University, West Lafayette, Indiana 47907, United States*
Annadka Shrinidhi − *Borch Department of Medicinal Chemistry and Molecular Pharmacology, College of Pharmacy, Purdue University, West Lafayette, Indiana 47907, United States;* orcid.org/0000-0003-1022-617X
Abdallah S. Abdelsattar − *Department of Biomedical Sciences and Pathobiology, Virginia-Maryland College of Veterinary Medicine, Virginia Polytechnic Institute and State University, Blacksburg, Virginia 24061, United States; Center for One Health Research, Virginia Polytechnic Institute and State University, Blacksburg, Virginia 24061, United States*
Victoria Burgo − *Duchossois Family Institute, University of Chicago, Chicago, Illinois 60637, United States*
Glory Melotte − *Duchossois Family Institute, University of Chicago, Chicago, Illinois 60637, United States*
Tomi Akin-Olabiyi − *Duchossois Family Institute, University of Chicago, Chicago, Illinois 60637, United States*
Sean Knoblauch − *Duchossois Family Institute, University of Chicago, Chicago, Illinois 60637, United States*
Ramanujam Ramaswamy − *Duchossois Family Institute, University of Chicago, Chicago, Illinois 60637, United States;* orcid.org/0000-0001-7448-6574
Che Woodson − *Duchossois Family Institute, University of Chicago, Chicago, Illinois 60637, United States*
Venkatesh P. Thirumalaikumar − *Purdue Proteomics Facility, Bindley Bioscience Center and Center for Plant Biology, Department of Botany and Plant Pathology, Purdue University, West Lafayette, Indiana 47907, United States*
J. Alejandra Rodriguez − *Department of Biological Sciences, Purdue University, West Lafeyette, Indiana 47907, United States*
Franklin J. Yeo − *Department of Biological Sciences, Purdue University, West Lafeyette, Indiana 47907, United States*
Olivia C. Snell − *Borch Department of Medicinal Chemistry and Molecular Pharmacology, College of Pharmacy, Purdue University, West Lafayette, Indiana 47907, United States*
Alessio Nocentini − *Department of Neurofarba, Section of Pharmaceutical and Nutraceutical Sciences, University of Florence, Sesto Fiorentino 50122, Italy;* orcid.org/0000-0003-3342-702X
Anitha Sundararajan − *Duchossois Family Institute, University of Chicago, Chicago, Illinois 60637, United States*
Matthew R. Olson − *Department of Biological Sciences, Purdue University, West Lafeyette, Indiana 47907, United States*
Claudiu T. Supuran − *Department of Neurofarba, Section of Pharmaceutical and Nutraceutical Sciences, University of Florence, Sesto Fiorentino 50122, Italy;* orcid.org/0000-0003-4262-0323

Complete contact information is available at: https://pubs.acs.org/10.1021/acsinfecdis.5c00736

Author Contributions

[#]N.S.A. and K.J.H. contributed equally.

Notes

The authors declare no competing financial interest.

■ ACKNOWLEDGMENTS

The authors would like to acknowledge research support and space provided by the Purdue College of Pharmacy to make this work possible. The Table of Contents graphic was made using BioRender.com through a license provided by Purdue College of Pharmacy. We thank the BEI Resources for supplying several of the clinical isolates used in this study. This work was funded by the Purdue College of Pharmacy (D.P.F.) and the Purdue Institute for Drug Discovery Program Grant (D.P.F. and M.N.S.), Drug Evaluation Committee Grant (D.P.F.), and the Chip and Jane Rutledge donation to the College of Pharmacy (D.P.F.). Research reported in this publication was supported by the National Institute of Allergy and Infectious Diseases of the National Institutes of Health under Award Numbers 1R01AI153264 (D.P.F. and M.N.S.) and 1R01AI148523 (D.P.F. and M.N.S.). The content is solely the responsibility of the authors and does not necessarily represent the official views of the National Institutes of Health. The authors thank the Bindley Bioscience Center for supporting the proteomics study. The proteomics work was supported by the Bindley method development pilot grant (D.P.F. and V.P.T.K.). Research from the Supuran lab was financed by the Italian Ministry for University Research (MIUR) and EU grants (EU-Horizon 2020, the Project Springboard Grant agreement No. 951883; project FISR2019_04819 BacCAD, MIUR). Figure 2 and the Table of Contents graphic were created with BioRender.com.

■ ABBREVIATIONS

ACN,acetonitrile; ADME,Absorption, Distribution, Metabolism, Excretion; APCI,atmospheric pressure chemical ionization; AUC,area under the curve; AZM,acetazolamide; BOP,benzotriazol-1-yloxytris(dimethylamino)phosphonium hexafluorophosphate; CA,carbonic anhydrase; CAI,carbonic anhydrase inhibitor; CFU,colony forming unit; C_{max},maximum concentration; CO2,carbon dioxide; DCM,dichloromethane; DIC,dissolved inorganic carbon; DIPEA,diisopropylethylamine; DMA,N,N-dimethylacetamide; DMSO,dimethyl sulfoxide; DNA,DNA; DTT,dithiothrietol; *Efα*-CA,*E. faecium α*-carbonic anhydrase; *Efγ*-CA,*E. faecium γ*-carbonic anhydrase; ESI,electrospray ionization; FA,formic acid; f_u,fraction unbound; GIT,gastrointestinal tract; hCA 1,human carbonic anhydrase 1; hCA 2,human carbonic anhydrase 2; HCl,hydrochloric acid; HPLC,high performance liquid chromatography; IAM,iodoacetamide; IV,intravenous; K_i,inhibition constant; LC-MS/MS,liquid chromatography tandem mass spectrometry; mCA 2,murine carbonic anhydrase 2; MeOH,-methanol; MIC,minimum inhibitory concentration; MLM,mouse liver microsome; MW,molecular weight; NaCl,-sodium chloride; NaOH,sodium hydroxide; P_{app},apparent

permeability; NMR,nuclear magnetic resonance; ODS,octadecylsilyl; PBS,phosphate buffered saline; PEG,polyethylene glycol; PK,pharmacokinetic; PO,per os; PPB,plasma protein binding; QD,quaque die; RBC,red blood cell; qPCR,quantitative polymerase chain reaction; RNA,ribonucleic acid; rRNA,ribosomal ribonucleic acid; SGF,simulated gastric fluid; SIF,simulated intestinal fluid; TBS,tris buffered saline; TFA,trifluoroacetic acid; TSB,tryptic soy broth; TMS,trimethylsilane; VRE,vancomycin-resistant Enterococci; WT,wild-type.

REFERENCES

(1) *Antibiotic Resistance Threats in the United States, 2019. U.S. Department of Health and Human Services, CDC*. 2019. https://www.cdc.gov/drugresistance/pdf/threats-report/2019-ar-threats-report-508.pdf.

(2) *HAI Pathogens and Antimicrobial Resistance Report; 2018−2021. U.S. Department of Health and Human Services, CDC*. **2023**. https://www.cdc.gov/nhsn/hai-report/index.html.

(3) Jeong, H.; Kang, S.; Cho, H. J. Prevalence of Multidrug-Resistant Organisms and Risk Factors for Carriage among Patients Transferred from Long-Term Care Facilities. *Infect. Chemother.* **2020**, *52* (2), 183−193.

(4) Rodríguez-Villodres, Á.; Martín-Gandul, C.; Peñalva, G.; Guisado-Gil, A. B.; Crespo-Rivas, J. C.; Pachón-Ibáñez, M. E.; Lepe, J. A.; Cisneros, J. M. Prevalence and Risk Factors for Multidrug-Resistant Organisms Colonization in Long-Term Care Facilities around the World: A Review. *Antibiotics* **2021**, *10* (6), 680.

(5) Eichel, V. M.; Last, K.; Brühwasser, C.; von Baum, H.; Dettenkofer, M.; Götting, T.; Grundmann, H.; Güldenhöven, H.; Liese, J.; Martin, M.; Papan, C.; Sadaghiani, C.; Wendt, C.; Werner, G.; Mutters, N. T. Epidemiology and Outcomes of Vancomycin-Resistant Enterococcus Infections: A Systematic Review and Meta-Analysis. *J. Hosp. Infect.* **2023**, *141*, 119−128.

(6) Ubeda, C.; Taur, Y.; Jenq, R. R.; Equinda, M. J.; Son, T.; Samstein, M.; Viale, A.; Socci, N. D.; Van Den Brink, M. R. M.; Kamboj, M.; Pamer, E. G. Vancomycin-Resistant Enterococcus Domination of Intestinal Microbiota Is Enabled by Antibiotic Treatment in Mice and Precedes Bloodstream Invasion in Humans. *J. Clin. Invest.* **2010**, *120* (12), 4332−4341.

(7) Donskey, C. J.; Chowdhry, T. K.; Hecker, M. T.; Hoyen, C. K.; Hanrahan, J. A.; Hujer, A. M.; Hutton-Thomas, R. A.; Whalen, C. C.; Bonomo, R. A.; Rice, L. B. Effect of Antibiotic Therapy on the Density of Vancomycin-Resistant Enterococci in the Stool of Colonized Patients. *N. Engl. J. Med.* **2000**, *343* (26), 1925−1932.

(8) McKinnell, J. A.; Arias, C. A. Linezolid vs Daptomycin for Vancomycin-Resistant Enterococci: The Evidence Gap between Trials and Clinical Experience. *Clin. Infect. Dis.* **2015**, *61* (6), 879−882.

(9) Bressler, A. M.; Zimmer, S. M.; Gilmore, J. L.; Somani, J. Peripheral Neuropathy Associated with Prolonged Use of Linezolid. *Lancet Infect. Dis.* **2004**, *4* (8), 528−531.

(10) Nowakowska, J.; Cameron, D. R.; De Martino, A.; Kühn, J.; Le Fresne-Languille, S.; Leuillet, S.; Amouzou, Y.; Wittke, F.; Carton, T.; Le Vacon, F.; Chaves, R. L.; Nicolas-Metral, V.; Vuagniaux, G. Evaluation of the Microbiota-Sparing Properties of the Anti-Staphylococcal Antibiotic Afabicin. *J. Antimicrob. Chemother.* **2023**, *78* (8), 1900−1908.

(11) Kandalai, S.; Li, H.; Zhang, N.; Peng, H.; Zheng, Q. The Human Microbiome and Cancer: A Diagnostic and Therapeutic Perspective. *Cancer Biol. Ther.* **2023**, *24* (1), No. 2240084.

(12) Stein-Thoeringer, C. K.; Saini, N. Y.; Zamir, E.; Blumenberg, V.; Schubert, M. L.; Mor, U.; Fante, M. A.; Schmidt, S.; Hayase, E.; Hayase, T.; Rohrbach, R.; Chang, C. C.; McDaniel, L.; Flores, I.; Gaiser, R.; Edinger, M.; Wolff, D.; Heidenreich, M.; Strati, P.; Nair, R.; Chihara, D.; Fayad, L. E.; Ahmed, S.; Iyer, S. P.; Steiner, R. E.; Jain, P.; Nastoupil, L. J.; Westin, J.; Arora, R.; Wang, M. L.; Turner, J.; Menges, M.; Hidalgo-Vargas, M.; Reid, K.; Dreger, P.; Schmitt, A.; Müller-Tidow, C.; Locke, F. L.; Davila, M. L.; Champlin, R. E.; Flowers, C. R.; Shpall, E. J.; Poeck, H.; Neelapu, S. S.; Schmitt, M.; Subklewe, M.; Jain, M. D.; Jenq, R. R.; Elinav, E. A Non-Antibiotic-Disrupted Gut Microbiome Is Associated with Clinical Responses to CD19-CAR-T Cell Cancer Immunotherapy. *Nat. Med.* **2023**, *29* (4), 906−916.

(13) Loh, J. S.; Mak, W. Q.; Tan, L. K. S.; Ng, C. X.; Chan, H. H.; Yeow, S. H.; Foo, J. B.; Ong, Y. S.; How, C. W.; Khaw, K. Y. Microbiota−Gut−Brain Axis and Its Therapeutic Applications in Neurodegenerative Diseases. *Signal Transduction Targeted Ther.* **2024**, *9* (1), 29−39.

(14) Schloissnig, S.; Arumugam, M.; Sunagawa, S.; Mitreva, M.; Tap, J.; Zhu, A.; Waller, A.; Mende, D. R.; Kultima, J. R.; Martin, J.; Kota, K.; Sunyaev, S. R.; Weinstock, G. M.; Bork, P. Genomic Variation Landscape of the Human Gut Microbiome. *Nature* **2013**, *493* (7430), 45−50.

(15) Zhang, L.; Liu, J.; Deng, M.; Chen, X.; Jiang, L.; Zhang, J.; Tao, L.; Yu, W.; Qiu, Y. Enterococcus Faecalis Promotes the Progression of Colorectal Cancer via Its Metabolite: Biliverdin. *J. Transl. Med.* **2023**, *21* (1), 72.

(16) Manfredo Vieira, S.; Hiltensperger, M.; Kumar, V.; Zegarra-Ruiz, D.; Dehner, C.; Khan, N.; Costa, F. R. C.; Tiniakou, E.; Greiling, T.; Ruff, W.; Barbieri, A.; Kriegel, C.; Mehta, S. S.; Knight, J. R.; Jain, D.; Goodman, A. L.; Kriegel, M. A. Translocation of a Gut Pathobiont Drives Autoimmunity in Mice and Humans. *Science* **2018**, *359* (6380), 1156−1161.

(17) Smith, A. B.; Jenior, M. L.; Keenan, O.; Hart, J. L.; Specker, J.; Abbas, A.; Rangel, P. C.; Di, C.; Green, J.; Bustin, K. A.; Gaddy, J. A.; Nicholson, M. R.; Laut, C.; Kelly, B. J.; Matthews, M. L.; Evans, D. R.; Van Tyne, D.; Furth, E. E.; Papin, J. A.; Bushman, F. D.; Erlichman, J.; Baldassano, R. N.; Silverman, M. A.; Dunny, G. M.; Prentice, B. M.; Skaar, E. P.; Zackular, J. P. Enterococci Enhance Clostridioides Difficile Pathogenesis. *Nature* **2022**, *611* (7937), 780−786.

(18) Lange, K.; Buerger, M.; Stallmach, A.; Bruns, T. Effects of Antibiotics on Gut Microbiota. *Dig. Dis.* **2016**, *34* (3), 260−268.

(19) Taur, Y.; Coyte, K.; Schluter, J.; Robilotti, E.; Figueroa, C.; Gjonbalaj, M.; Littmann, E. R.; Ling, L.; Miller, L.; Gyaltshen, Y.; Fontana, E.; Morjaria, S.; Gyurkocza, B.; Perales, M. A.; Castro-Malaspina, H.; Tamari, R.; Ponce, D.; Koehne, G.; Barker, J.; Jakubowski, A.; Papadopoulos, E.; Dahi, P.; Sauter, C.; Shaffer, B.; Young, J. W.; Peled, J.; Meagher, R. C.; Jenq, R. R.; Van Den Brink, M. R. M.; Giralt, S. A.; Pamer, E. G.; Xavier, J. B. Reconstitution of the Gut Microbiota of Antibiotic-Treated Patients by Autologous Fecal Microbiota Transplant. *Sci. Transl. Med.* **2018**, *10* (460), 1−8.

(20) Muñoz, K. A.; Ulrich, R. J.; Vasan, A. K.; Sinclair, M.; Wen, P.; Holmes, J. R.; Lee, H. Y.; Hung, C.; Fields, C. J.; Tajkhorshid, E.; Lau, G. W.; Hergenrother, P. J. A Gram-Negative-Selective Antibiotic That Spares the Gut Microbiome. *Nature* **2024**, *630* (8016), 429−436.

(21) Leimer, N.; Wu, X.; Imai, Y.; Morrissette, M.; Pitt, N.; Favre-Godal, Q.; Iinishi, A.; Jain, S.; Caboni, M.; Leus, I. V.; Bonifay, V.; Niles, S.; Bargabos, R.; Ghiglieri, M.; Corsetti, R.; Krumpoch, M.; Fox, G.; Son, S.; Klepacki, D.; Polikanov, Y. S.; Freliech, C. A.; McCarthy, J. E.; Edmondson, D. G.; Norris, S. J.; D'Onofrio, A.; Hu, L. T.; Zgurskaya, H. I.; Lewis, K. A Selective Antibiotic for Lyme Disease. *Cell* **2021**, *184* (21), 5405−5418.e16.

(22) Supuran, C. T. Carbonic Anhydrases: Novel Therapeutic Applications for Inhibitors and Activators. *Nat. Rev. Drug. Discovery* **2008**, *7* (2), 168−181.

(23) Capasso, C.; Supuran, C. T. Bacterial, Fungal and Protozoan Carbonic Anhydrases as Drug Targets. *Expert Opin. Ther. Targets* **2015**, *19* (12), 1689−1704.

(24) Flaherty, D. P.; Seleem, M. N.; Supuran, C. T. Bacterial Carbonic Anhydrases: Underexploited Antibacterial Therapeutic Targets. *Future Med. Chem.* **2021**, *13* (19), 1619−1622.

(25) Aspatwar, A.; Tolvanen, M. E. E.; Parkkila, S. Phylogeny and Expression of Carbonic Anhydrase-Related Proteins. *BMC Mol. Biol.* **2010**, *11*, 25.

(26) Ritschel, W. A.; Paulos, C.; Arancibia, A.; Agrawal, M. A.; Wetzelsberger, K. M.; Lücker, P. W. Pharmacokinetics of

Acetazolamide in Healthy Volunteers after Short-and Long-term Exposure to High Altitude. *J. Clin. Pharmacol.* **1998**, *38* (6), 533−539.
(27) Loiselle, A. R.; de Kleine, E.; van Dijk, P.; Jansonius, N. M. Intraocular and Intracranial Pressure in Glaucoma Patients Taking Acetazolamide. *PLoS One* **2020**, *15* (6), No. e0234690.
(28) Kaunisto, K.; Parkkila, S.; Rajaniemi, H.; Waheed, A.; Grubb, J.; Sly, W. S. Carbonic Anhydrase XIV: Luminal Expression Suggests Key Role in Renal Acidification. *Kidney Int.* **2002**, *61* (6), 2111−2118.
(29) Kaur, J.; Cao, X.; Abutaleb, N. S.; Elkashif, A.; Graboski, A. L.; Krabill, A. D.; AbdelKhalek, A. H.; An, W.; Bhardwaj, A.; Seleem, M. N.; Flaherty, D. P. Optimization of Acetazolamide-Based Scaffold as Potent Inhibitors of Vancomycin-Resistant Enterococcus. *J. Med. Chem.* **2020**, *63* (17), 9540−9562.
(30) An, W.; Holly, K. J.; Nocentini, A.; Imhoff, R. D.; Hewitt, C. S.; Abutaleb, N. S.; Cao, X.; Seleem, M. N.; Supuran, C. T.; Flaherty, D. P. Structure-Activity Relationship Studies for Inhibitors for Vancomycin-Resistant Enterococcus and Human Carbonic Anhydrases. *J. Enzyme Inhib. Med. Chem.* **2022**, *37* (1), 1838−1844.
(31) Ammara, A.; Giovannuzzi, S.; Bonardi, A.; Abutaleb, N. S.; Abouelkhair, A. A.; Flaherty, D. P.; Seleem, M. N.; Capasso, C.; Gratteri, P.; Nocentini, A.; Supuran, C. T. Redesigning Oxazolidinones as Carbonic Anhydrase Inhibitors against Vancomycin-Resistant Enterococci. *Eur. J. Med. Chem.* **2025**, *291*, No. 117620.
(32) Holly, K. J.; Youse, M. S.; Flaherty, D. P. Enterococci Carbonic Anhydrase Inhibition. In *Enzymes*; Elsevier, 2024; pp 1−29.
(33) Abutaleb, N. S.; Elhassanny, A. E. M.; Flaherty, D. P.; Seleem, M. N. In Vitro and in Vivo Activities of the Carbonic Anhydrase Inhibitor, Dorzolamide, against Vancomycin-Resistant Enterococci. *PeerJ.* **2021**, *9*, No. e11059.
(34) Holly, K. J.; Tharra, P. R.; Abutaleb, N. S.; Nocentini, A.; Abouelkhair, A. A.; Youse, M. S.; Marapaka, A. K.; Abdelsattar, A. S.; An, W.; Drummond, F. L.; Snell, O. C.; Supuran, C. T.; Seleem, M. N.; Flaherty, D. P. Hit-to-Lead Optimization of Acetazolamide-Based Bacterial Carbonic Anhydrase Inhibitors with Efficacy In Vivo for Treatment of Vancomycin-Resistant Enterococci Septicemia. *J. Med. Chem.* **2025**, *68* (17), 18597−18624.
(35) Youse, M. S.; Holly, K. J.; Flaherty, D. P. Neisseria Gonorrhoeae Carbonic Anhydrase Inhibition. In *The Enzymes*; Elsevier, 2024; pp 1−39.
(36) Giovannuzzi, S.; Abutaleb, N. S.; Hewitt, C. S.; Carta, F.; Nocentini, A.; Seleem, M. N.; Flaherty, D. P.; Claudiu, T.; Nocentini, A.; Seleem, M. N.; Flaherty, D. P.; Supuran, C. T. Dithiocarbamates Effectively Inhibit the α -Carbonic Anhydrase from Neisseria Gonorrhoeae Gonorrhoeae. *J. Enzyme Inhib. Med. Chem.* **2022**, *37* (1), 1−8.
(37) Youse, M. S.; Abutaleb, N. S.; Nocentini, A.; S Abdelsattar, A.; Ali, F.; Supuran, C. T.; Seleem, M. N.; Flaherty, D. P. Optimization of Ethoxzolamide Analogs with Improved Pharmacokinetic Properties for In Vivo Efficacy against Neisseria Gonorrhoeae. *J. Med. Chem.* **2024**, *67* (17), 15537−15556.
(38) Hewitt, C. S.; Abutaleb, N. S.; Elhassanny, A. E. M.; Nocentini, A.; Cao, X.; Amos, D. P.; Youse, M. S.; Holly, K. J.; Marapaka, A. K.; An, W.; Kaur, J.; Krabill, A. D.; Elkashif, A.; Elgammal, Y.; Graboski, A. L.; Supuran, C. T.; Seleem, M. N.; Flaherty, D. P. Structure-Activity Relationship Studies of Acetazolamide-Based Carbonic Anhydrase Inhibitors with Activity against Neisseria Gonorrhoeae. *ACS Infect. Dis.* **2021**, *7* (7), 1969−1984.
(39) Marapaka, A. K.; Nocentini, A.; Youse, M. S.; An, W.; Holly, K. J.; Das, C.; Yadav, R.; Seleem, M. N.; Supuran, C. T.; Flaherty, D. P. Structural Characterization of Thiadiazolesulfonamide Inhibitors Bound to Neisseria Gonorrhoeae α-Carbonic Anhydrase. *ACS Med. Chem. Lett.* **2023**, *14* (1), 103−109.
(40) Abutaleb, N. S.; Shrinidhi, A.; Bandara, A. B.; Seleem, M. N.; Flaherty, D. P. Evaluation of 1,3,4-Thiadiazole Carbonic Anhydrase Inhibitors for Gut Decolonization of Vancomycin-Resistant Enterococci. *ACS Med. Chem. Lett.* **2023**, *14*, 487−492.
(41) Abutaleb, N. S.; Elkashif, A.; Flaherty, D. P.; Seleem, M. N. In Vivo Antibacterial Activity of Acetazolamide. *Antimicrob. Agents Chemother.* **2021**, *65*, e01715−e01720.
(42) Choi, P. H.; Jo, J.; Lin, Y. C.; Lin, M. H.; Chou, C. Y.; Dietrich, L. E. P.; Tong, L. A Distinct Holoenzyme Organization for Two-Subunit Pyruvate Carboxylase. *Nat. Commun.* **2016**, *7*, 7.
(43) Freiberg, C.; Brunner, N. A.; Schiffer, G.; Lampe, T.; Pohlmann, J.; Brands, M.; Raabe, M.; Häbich, D.; Ziegelbauer, K. Identification and Characterization of the First Class of Potent Bacterial Acetyl-CoA Carboxylase Inhibitors with Antibacterial Activity. *J. Biol. Chem.* **2004**, *279* (25), 26066−26073.
(44) Dong, H.; Cronan, J. E. Unsaturated Fatty Acid Synthesis in Enterococcus Faecalis Requires a Specific Enoyl-ACP Reductase. *Mol. Microbiol.* **2022**, *118* (5), 541−551.
(45) Ayoub, N.; Gedeon, A.; Munier-Lehmann, H. A Journey into the Regulatory Secrets of the de Novo Purine Nucleotide Biosynthesis. *Front. Pharmacol.* **2024**, *15*, No. 1329011.
(46) Merlin, C.; Masters, M.; McAteer, S.; Coulson, A. Why Is Carbonic Anhydrase Essential to Escherichia Coli? *J. Bacteriol.* **2003**, *185* (21), 6415−6424.
(47) Rubin, D. H. F.; Ma, K. C.; Westervelt, K. A.; Hullahalli, K.; Waldor, M. K.; Grad, Y. H. CanB Is a Metabolic Mediator of Antibiotic Resistance in Neisseria Gonorrhoeae. *Nat. Microbiol.* **2023**, *8* (1), 28−39.
(48) Fan, S.-H.; Ebner, P.; Reichert, S.; Hertlein, T.; Zabel, S.; Lankapalli, A. K.; Nieselt, K.; Ohlsen, K.; Götz, F. MpsAB Is Important for Staphylococcus Aureus Virulence and Growth at Atmospheric CO2 Levels. *Nat. Commun.* **2019**, *10* (1), 3627.
(49) Fan, S.; Matsuo, M.; Huang, L.; Tribelli, P. M. The MpsAB Bicarbonate Transporter Is Superior to Carbonic Anhydrase in Biofilm-Forming Bacteria with Limited CO2 Diffusion. *Microbiol. Spectrum* **2021**, *9* (1), No. e00305-21.
(50) Champney, W. S.; Miller, M. Linezolid Is a Specific Inhibitor of 50S Ribosomal Subunit Formation in Staphylococcus Aureus Cells. *Curr. Microbiol.* **2002**, *44* (5), 350−356.
(51) Fan, S.; Liberini, E.; Götz, F. Staphylococcus Aureus Genomes Harbor Only MpsAB-Like Dissolved Inorganic Carbon Supply System. *Microbiol. Spectrum* **2021**, *9*, No. e00970−21.
(52) Fan, S.; Matsuo, M.; Huang, L.; Tribelli, P. M.; Götz, F. The MpsAB Bicarbonate Transporter Is Superior to Carbonic Anhydrase in Biofilm-Forming Bacteria with Limited CO 2 Diffusion. *Microbiol. Spectrum* **2021**, *9* (1), No. e0030521.
(53) Fan, S.-H.; Proctor, R. A.; Ersoy, S. C.; Manna, A. C.; Cheung, A. L.; Götz, F.; Chambers, H. F.; Bayer, A. S. Role of the NaHCO 3 Transporter MpsABC in the NaHCO 3 − β-Lactam-Responsive Phenotype in Methicillin-Resistant Staphylococcus Aureus. *Microbiol. Spectrum* **2023**, *11* (3), No. e00141-23.
(54) Munckhof, W. J.; Giles, C.; Turnidge, J. D. Post-Antibiotic Growth Suppression of Linezolid against Gram-Positive Bacteria. *J. Antimicrob. Chemother.* **2001**, *47* (6), 879−883.
(55) Chilambi, G. S.; Wang, Y.; Wallace, N. R.; Obiwuma, C.; Evans, K. M.; Li, Y.; Shalaby, M. W.; Flaherty, D. P.; Shields, R. K.; Doi, Y.; Van Tyne, D. Carbonic Anhydrase Inhibition as a Target for Antibiotic Synergy in Enterococci. *Microbiol. Spectrum* **2023**, *11* (4), No. e03963-22.
(56) Leeson, P. D.; Springthorpe, B. The Influence of Drug-like Concepts on Decision-Making in Medicinal Chemistry. *Nat. Rev. Drug Discovery* **2007**, *6* (11), 881−890.
(57) Bednarczyk, D.; Sanghvi, M. V. The Impact of Assay Recovery on the Apparent Permeability, a Function of Lysosomal Trapping. *Xenobiotica* **2020**, *50* (7), 753−760.
(58) Wallace, S. M.; Riegelman, S. Uptake of Acetazolamide by Human Erythrocytes in Vitro. *J. Pharm. Sci.* **1977**, *66*, 729−731.
(59) Wallace, S. M.; Shah, V. P.; Riegelman, S. GLC Analysis of Acetazolamide in Blood, Plasma, and Saliva Following Oral Administration to Normal Subjects. *J. Pharm. Sci.* **1977**, *66* (4), 527−530.
(60) Thierfelder, W.; Cummings, P.; Fraser, P.; Curtis, P. J. Expression of Carbonic Anhydrases I and II in Mouse Erythropoiesis. In *The Carbonic Anhydrases*; Springer US: Boston, MA, 1991; pp 209−214.

(61) Ridderstråle, Y.; Wistrand, P. J. Membrane-Associated Carbonic Anhydrase Activity in the Brain of CA II-Deficient Mice. *J. Neurocytol.* **2000**, *29* (4), 263−269.
(62) Robert, X.; Gouet, P. Deciphering Key Features in Protein Structures with the New ENDscript Server. *Nucleic Acids Res.* **2014**, *42* (W1), W320−W324.
(63) Nti-Addae, K. W.; Guarino, V. R.; Dalwadi, G.; Stella, V. J. Determination of the Permeability Characteristics of Two Sulfenamide Prodrugs of Linezolid across Caco-2 Cells. *J. Pharm. Sci.* **2012**, *101* (9), 3134−3141.
(64) Beringer, P.; Nguyen, M.; Hoem, N.; Louie, S.; Gill, M.; Gurevitch, M.; Wong-Beringer, A. Absolute Bioavailability and Pharmacokinetics of Linezolid in Hospitalized Patients given Enteral Feedings. *Antimicrob. Agents Chemother.* **2005**, *49* (9), 3676−3681.
(65) Krause, A. L.; Stinear, T. P.; Monk, I. R. Barriers to Genetic Manipulation of Enterococci: Current Approaches and Future Directions. *FEMS Microbiol. Rev.* **2022**, *46* (6), 1−14.
(66) Krause, A. L.; Judd, L. M.; Wick, R.; Stinear, T. P.; Buultjens, A. H.; Monk, I. R. Comparative and Functional Genomic Analysis of Foreign DNA Defense Mechanisms in Enterococcus Faecium. *Microbiol. Spectrum* **2025**, *13* (8), No. e0028925.
(67) Levert, K. L.; Lloyd, R. B.; Waldrop, G. L. Do Cysteine 230 and Lysine 238 of Biotin Carboxylase Play a Role in the Activation of Biotin. *Biochemistry* **2000**, *39* (14), 4122−4128.
(68) Polyak, S. W.; Abell, A. D.; Wilce, M. C. J.; Zhang, L.; Booker, G. W. Structure, Function and Selective Inhibition of Bacterial Acetyl-Coa Carboxylase. *Appl. Microbiol. Biotechnol.* **2012**, *93* (3), 983−992.
(69) Mueller, E. J.; Meyer, E.; Rudolph, J.; Davisson, V. J.; Stubbe, J. A. N5-Carboxyaminoimidazole Ribonucleotide: Evidence for a New Intermediate and Two New Enzymatic Activities in the de Novo Purine Biosynthetic Pathway of Escherichia Coli. *Biochemistry* **1994**, *33* (8), 2269−2278.
(70) Remmele, C. W.; Xian, Y.; Albrecht, M.; Faulstich, M.; Fraunholz, M.; Heinrichs, E.; Dittrich, M. T.; Müller, T.; Reinhardt, R.; Rudel, T. Transcriptional Landscape and Essential Genes of Neisseria Gonorrhoeae. *Nucleic Acids Res.* **2014**, *42* (16), 10579−10595.
(71) Johnson, B. K.; Colvin, C. J.; Needle, D. B.; Mba Medie, F.; Champion, P. A. D. D.; Abramovitch, R. B. The Carbonic Anhydrase Inhibitor Ethoxzolamide Inhibits the Mycobacterium Tuberculosis PhoPR Regulon and Esx-1 Secretion and Attenuates Virulence. *Antimicrob. Agents Chemother.* **2015**, *59* (8), 4436−4445.
(72) Nishimori, I.; Onishi, S.; Takeuchi, H.; Supuran, C. The Alpha and Beta Classes Carbonic Anhydrases from Helicobacter Pylori as Novel Drug Targets. *Curr. Pharm. Des.* **2008**, *14* (7), 622−630.
(73) Marcus, E. A.; Moshfegh, A. P.; Sachs, G.; Scott, D. R. The Periplasmic A-Carbonic Anhydrase Activity of Helicobacter Pylori Is Essential for Acid Acclimation. *J. Bacteriol.* **2005**, *187* (2), 729−738.
(74) Colquhoun, J. M.; Farokhyfar, M.; Anderson, A. C.; Bethel, C. R.; Bonomo, R. A.; Clarke, A. J.; Rather, P. N. Collateral Changes in Cell Physiology Associated with ADC-7 β-Lactamase Expression in Acinetobacter Baumannii. *Microbiol. Spectrum* **2023**, *11* (3), No. e0464622.
(75) Ten Hove, M. W.; Friedman, D. I.; Patel, A. D.; Irrcher, I.; Wall, M.; McDermott, M. P. Safety and Tolerability of Acetazolamide in the Idiopathic Intracranial Hypertension Treatment Trial. *J. Neuro-Ophthalmol.* **2016**, *36* (1), 13−19.

https://doi.org/10.1021/acsinfecdis.5c00736
ACS Infect. Dis. 2026, 12, 176−189